

Synthesis and characterization of zinc AP-MOCVD precursors and their utility in the growth of ZnO

Jason S. Matthews,* Olamide O. Onakoya, Tantiboro S. Ouattara and Raymond J. Butcher

Received 6th March 2006, Accepted 28th April 2006

First published as an Advance Article on the web 10th May 2006

DOI: 10.1039/b603308c

A novel β -ketoimine, 4-*N*-(*n*-butylamino)-3-penten-2-one (**1**), and β -enaminoester, Ethyl 3-*N*-(isopropylamino)-2-butenate (**2**), were synthesized by the reaction of the 2,4-pentanedione or ethyl 3-oxo butanoate with the *n*-butyl and isopropyl amine, respectively. The isolated free ligands **1** and **2** were reacted with diethylzinc to afford $\text{Zn}(\text{CH}_3\text{C}(\text{NCH}_2\text{CH}_2\text{CH}_2\text{CH}_3)\text{CHCOCH}_3)_2$ (**3**) and $\text{Zn}(\text{CH}_3\text{C}(\text{NCH}(\text{CH}_3)_2)\text{CHC}(\text{O})\text{OCH}_2\text{CH}_3)_2$ (**4**) respectively. The isolated zinc complexes, **3** and **4**, were characterized by elemental analysis, NMR, and MALDI-TOFMS. The molecular structure of **3** and **4** were determined *via* single crystal X-ray diffraction which revealed both compounds to be four coordinate, monomeric and homoleptic in the solid state. TG analysis showed the air stable compounds to be thermally robust as they both sublimed in a one-step process at atmospheric pressure. The compounds were utilized in the growth of ZnO *via* AP-MOCVD in the absence of additional oxidant. The carbon content of the film grown from **3** as determined by XPS was 26.2% while that of the film grown by **4** was 8.71%.

Introduction

Metal–organic chemical vapor deposition (MOCVD) of ZnO has recently received significant attention. Applications of the wide band gap (3.37 eV) semiconductor, characterized by its large exciton binding energy of 60 meV, include blue and ultraviolet light-emitting and solar cell devices¹ as well as thin films for use as resistive gas sensors.² Zinc oxide also exhibits piezoelectric properties, making it useful in the fabrication of microsensor devices and micromachined actuators.³ Additional applications for ZnO based materials include optical waveguides⁴ and varistors.⁵ More recently, ZnO nanocolumns have been grown and their utility studied in the fabrication of field effect transistors.⁶ The growth of ZnO has been carried out *via* several different methods. These methods include chemical spray pyrolysis, atomic layer deposition, magnetron sputtering and MOCVD.^{7–14} Atmospheric pressure (AP) MOCVD has presented itself as the most promising method because of the capability for large area growth, precise control of film thickness, good conformal coverage, preferred orientation and high growth rates. In developing a suitable precursor for AP-MOCVD of ZnO, consideration of volatility, stability and the ability to deposit the desired material without carbon contamination is paramount.

The precursor chemistry for the preparation of ZnO *via* MOCVD includes metal alkyls like diethylzinc (DEZ) in combination with an oxygen source (*i.e.* H₂O or ROH).¹⁵ These systems, however, suffer from gas phase pre-reaction, resulting in precursor decomposition and film contamination. Based on the hypothesis that the DEZ/ROH system undergoes a gas phase reaction to form alkyl zinc alkoxides, the single source tetrameric precursors [MeZn(OPr^t)₄] and [MeZn(OBu^t)] were envisaged.

These compounds were synthesized and found to exhibit sufficient volatility and excellent thermal stability at reduced pressure and thus were successfully utilized in the low pressure (LP) MOCVD growth of ZnO.¹⁶ Our recent investigations into improving the behavior of MOCVD precursors have led us to the investigation of β -ketoiminate and β -iminoesterate ligand platforms. The β -ketoiminate ligand system has been previously studied for use in the CVD of main group, lanthanide and transition metal oxides^{17–27} and the β -ketoester platform has been utilized in the growth of ZrO₂ and TiO₂ for the fabrication of lead zirconium titanate.^{28,29} Marrying the structure of the β -ketoimine with that of the β -ketoester gives access to the β -enaminoester. We have begun to investigate utility of the β -iminoesterate ligand system in the preparation of novel ZnO precursors. Herein we describe the synthesis, characterization, thermal behavior and preliminary AP-MOCVD results of a zinc *bis* β -ketoiminate and a novel β -iminoesterate.

Results and discussion

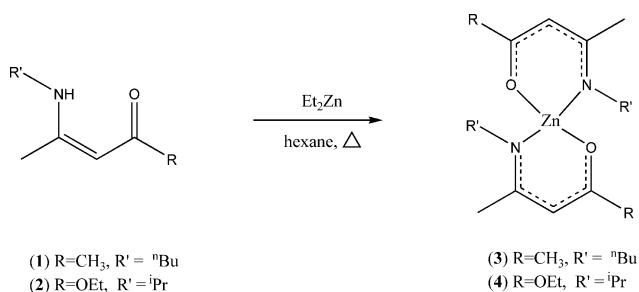
Precursor synthesis

The synthesis of the β -ketoimine **1** was carried out by the direct combination of 2,4-pentanedione and *n*-butylamine. The reagents were combined and refluxed for 1 h in diethyl ether. The crude product was distilled to afford **1** as a colorless oil. The synthesis of the β -enaminoester **2** was carried out utilizing a method similar to that described for **1** by reacting ethyl 3-oxobutanoate with isopropylamine. The isolated product was distilled under reduced pressure to afford **2** as a colorless oil. ¹H and ¹³C NMR and mass spectrometric data for **1** and **2** were consistent with the expected formulation.

The synthesis of **3** was carried out by the direct reaction of **1** with diethylzinc. The reaction mixture was heated to reflux for 30 min after which the solvent was removed *in vacuo* to afford **3**

Department of Chemistry, Howard University, 525 College Street, N.W. Washington DC, 20059, USA. E-mail: jsmatthews@howard.edu; Fax: +1-202-806-5442; Tel: +1-202-806-6892

as a white solid. Sublimation of the crude product gave a white powdery material that was characterized by NMR. The proton resonances were shifted slightly downfield from that of the free ligand **1** and the spectra did not contain the *NH* resonance at δ 10.88 indicating that the sublimed material did not contain unreacted free ligand. The synthesis of **4** was carried out in a similar fashion to that of **3**. The reaction of **2** with diethylzinc afforded a viscous liquid upon removal of the solvent. Pentane was added to the reaction product and the solution was cooled to -5°C overnight resulting in the formation of a white precipitate. The solvent was removed *via* cannula and the precipitate was washed several times with cold pentane. The product was dried *in vacuo* and sublimed under reduced pressure to afford a white crystalline powder that was characterized *via* NMR revealing spectroscopic data corresponding to **4**.



Scheme 1 Synthetic scheme for the preparation of complexes **3** and **4**.

Physical characterization

Mass spectral analysis of sublimed **3** and **4** was carried out *via* MALDI-TOFMS. The method for MS analysis was the same for both compounds. The matrix, *meso* tetrakis(pentafluoro-phenyl) porphyrin (F20TPP), was combined with the metal complex to form a solution. A portion of the solution was placed onto a steel MALDI sample plate and the resultant residue was characterized.

The mass spectrum of **3** contained the expected molecular ion, m/z 373.21 as part of a series of seven peaks of differing intensities due to the isotopes of zinc and carbon. The ion at m/z 373.21 was due to ^{64}Zn which has a natural abundance of 49%, the ion at m/z 375.21 corresponded to ^{66}Zn -28% while the ion at m/z 377.35 was due to ^{68}Zn -19%. The mass spectrum for **4** contained the expected molecular ion, m/z 404.23, along with the expected isotopic pattern consisting of m/z 406.25 and m/z 408.21.

Crystals of **3** and **4** suitable for single crystal X-ray diffraction studies were obtained by dissolving the isolated product in the minimum amount of hexane and cooling to -5°C for several days. The crystal structure of **3** reveals a four coordinate zinc center residing in a slightly distorted tetrahedral environment. The Zn–O bond lengths were 1.942 Å and 1.945 Å while the Zn–N bond distances are slightly longer at 1.984 Å and 1.989 Å. This difference is due to the fact that the electrons are not fully delocalized about the six membered chelate. The bond angles about the tetrahedral zinc center range from 98.11–121.64°, deviating from that of an ideal tetrahedron. The observed N–Zn–O bite angles were 98.11° and 98.37°.

The solid-state structure of **4** also revealed a distorted tetrahedral environment. The Zn–N distances were 1.948 Å and 1.949 Å

while the Zn–O distances were 1.945 Å and 1.957 Å. The bond angles about the zinc center range from 96.64–129.30° with N–Zn–O bite angles of 96.64° and 97.85°. These bond angles are smaller than those observed for **3**. Further comparison of the two structures show that the Zn–N and Zn–O bond lengths in **3** differ by approximately 0.040 Å while the analogous bonds in **4** differ by only 0.002 Å. The small difference between the Zn–N and Zn–O bond lengths in **4** is quite unprecedented for similar asymmetric β -difunctional chelating ligand systems. This anomaly can be attributed to the electron donating ethoxy group which is absent from **3**. The coordinating N and O atoms of β -ketoiminates generally bind to metal centers in an inequivalent fashion due in part to the competition between N and O atoms for electron density. This results in the electronegative oxygen forming an ionic bond with the metal center while nitrogen forms a weaker dative bond. Asymmetric bonding of the β -ketoiminate's coordinating N and O atoms to the metal center has been shown to contribute significantly to the non-intact atmospheric pressure sublimation of the heavy group 2 metal β -ketoiminates.³⁰

Thermal analysis

Thermogravimetric analysis carried out on **3** and **4** is shown in Fig. 3. Both compounds are volatilized in a one step process and exhibit minimal or no decomposition thus supporting their potential utility as viable AP-MOCVD precursors. Both **3** and **4** are low melting solids with mp of 72 and 109 °C, respectively. The compounds melt prior to vaporization with the onset for **3** being 150 °C while that of **4** is significantly higher at 250 °C. Compound **4** sublimed without decomposition as evidenced by the lack of residue remaining in the TG sample pan. The TG analysis of **3**, however, resulted in a 2% residue at the end of the vaporization process.

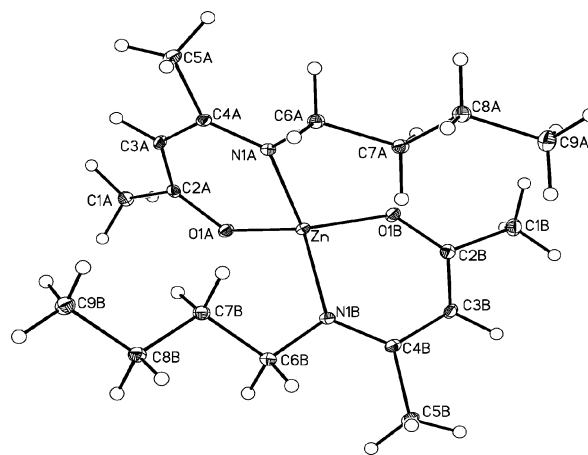


Fig. 1 Molecular structure of **3** showing thermal ellipsoids at the 50% probability level.

AP-MOCVD and film characterization

Preliminary AP-MOCVD experiments were carried out using a hot-walled CVD reactor comprising a quartz tube and a tube furnace.²³ The precursors were loaded into a porcelain boat at the front of the quartz tube and heated to either 205 °C or 225 °C under a flow of N_2 . The Si substrates were loaded into the quartz tube

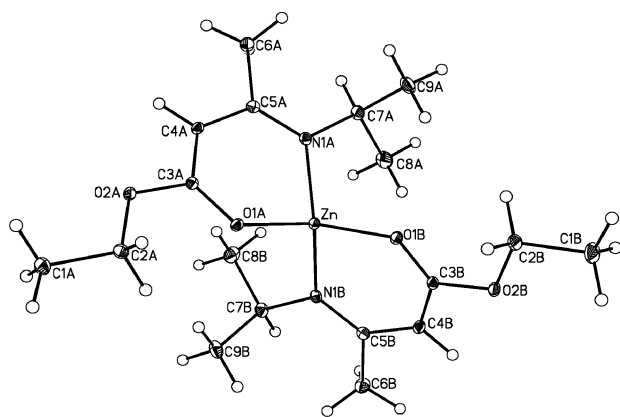


Fig. 2 Molecular structure of **4** showing thermal ellipsoids at the 50% probability.

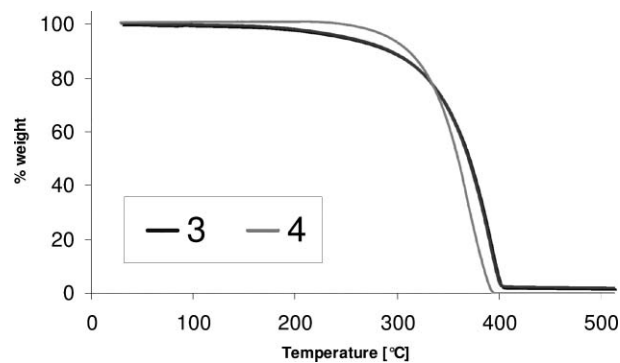


Fig. 3 TG Plot of **3** and **4**.

and heated to 450 °C. The deposition was carried out for 120 min during which time the substrates were coated with a thin film of ZnO. The films were crystalline as confirmed by XRD analysis which revealed that there was a strong preferential orientation in the (110) direction when **3** and **4** were utilized as precursors (Fig. 4). XPS analysis showed that precursor selection greatly affects the composition of the desired film. The thin film grown from **3** had an atomic carbon content of 26.2% while that grown from **4** was 8.7%. We believe this to be due primarily to the ethoxy oxygen atom which serves as an intrinsic oxidant facilitating the growth of ZnO.

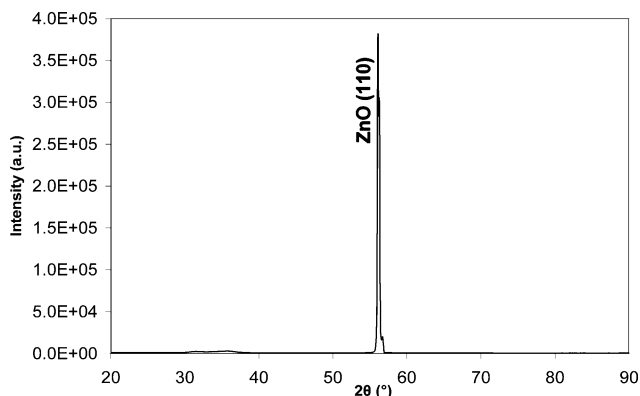


Fig. 4 XRD diagram of as deposited ZnO utilizing **4**.

Conclusions

Two novel ZnO AP-MOCVD precursors were synthesized and structurally characterized. The compounds, $[\text{Zn}(\text{CH}_3\text{C}(\text{NCH}_2\text{CH}_2\text{CH}_2\text{CH}_3)\text{CHCOCH}_3)_2]$ (**3**) and $[\text{Zn}(\text{CH}_3\text{C}(\text{NCH}(\text{CH}_3)_2)\text{CHC}(\text{O})\text{OCH}_2\text{CH}_3)_2]$ (**4**) are thermally robust and air stable. The volatility of **3** and **4** as determined by TG analysis showed both precursors to sublime *via* a one step process. Both precursors are low melting solids and were utilized in the CVD growth of crystalline ZnO at atmospheric pressure in the absence of added oxidant. The carbon content of the films grown utilizing **3** and **4** was examined *via* XPS. The film grown from **3** contained 26.2% carbon and the film grown from **4** contained 8.7% carbon. The high carbon content of the film grown from **3** can be attributed to premature decomposition of the precursor during the volatilization process as evidenced by the initial weight loss during the TG analysis and incomplete precursor decomposition during the deposition process. The significant reduction in carbon content in the film grown from **4** is due to the presence of the ethoxy moiety which makes available an additional oxygen source facilitating the deposition of ZnO. The incorporation of additional oxygen atoms into the precursor can therefore serve as an alternative to film growth in the presence of an oxidant like O_2 as is the current practice with precursors of this type.^{20,31,32} The ethoxy moiety also affects the manner in which the ligand binds to the zinc center. Generally, β -ketoiminates form ionic bonds to metal centers through the oxygen atom while the nitrogen atom forms a significantly weaker dative bond as evidenced by the solid state structure of **3**. However, the crystal structure of **4** reveals that there is sufficient electron density in the chelate ring, resulting in similar bond lengths for Zn–O and Zn–N. The weak M–N bond that is often observed for metal β -ketoiminates has been shown to contribute to reduced thermal stability of the precursor as evidenced in TG analysis of the heavy group 2 complexes.³⁰ Further investigation of the β -iminoesterate ligand system could potentially lead to improved precursors for the heavy group 2 metals. Additionally, the incorporation of additional oxygen atoms into the ligand should further reduce amount of carbon incorporated into the thin film when the growth process is carried out in the absence of oxygen.

Experimental

General procedures

All manipulations were carried out in oven dried glassware under a dry nitrogen atmosphere using standard Schlenk techniques. Pentane, hexane and diethyl ether were freshly distilled from sodium benzophenone ketyl. Ethyl 3-oxobutanoate (EM Science) and 2,4-pentanedione (Aldrich) were purchased and distilled prior to use. All other reagents were purchased from Aldrich and used without further purification.

Physical measurements

^1H and ^{13}C NMR spectra were recorded with a Bruker AVANCE 400 MHz Ultra Shield™ NMR spectrometer. Chemical shifts for ^1H (400 MHz) and ^{13}C (100 MHz) were referenced to CDCl_3 and reported in ppm. Mass Spectra were collected using a Agilent Technologies 5973 *inert* Mass Selective Detector.

MALDI-TOFMS analyses were carried out using a Perkin Elmer Voyager-DE STR Biospectrometry workstation equipped with a two-stage acceleration source. FT-IR spectra were collected using a Nicolet MAGNA-IR 560 spectrometer (E.S.P). Thermal analyses were carried out on a Perkin-Elmer thermogravimetric analyzer series 7 under a nitrogen atmosphere at 1 atm. The thermogram was obtained from samples weighing 3–5 mg with heating at a rate of 20 °C min⁻¹. Elemental analyses were performed on a Perkin-Elmer PE2400 microanalyzer. X-Ray powder diffraction studies were conducted on a Bruker AXS D8 diffractometer using monochromated Cu-K α radiation. The samples were mounted flat and scanned from 5 to 95° in a step size of 0.04° with a count rate of 2.5 s.

Synthesis

[CH₃C(NCH₂CH₂CH₂CH₃)CH₂COCH₃] (1). To a solution of 2, 4-pentanedione (11.44 g, 114.26 mmol) in diethyl ether (30 mL) was added *n*-butylamine (8.5 g, 116.21 mmol). The resulting solution was refluxed for 1 h at room temperature under stirring. After cooling, an additional 20 mL of diethyl ether was added and the solution was dried over magnesium sulfate. After filtration and removal of the solvent, the product was purified by reduced pressure distillation to afford **1** as a light yellow viscous liquid (15.9 g, 89.8% yield). bp (102 °C, 6 mmHg). ¹H NMR (400 MHz, CDCl₃) δ_{H} 0.80 (t, 3H, CH₃CH₂), 1.27 (m, 2H, CH₃CH₂CH₂), 1.42 (m, 2H, CH₂CH₂CH₂), 1.78 (s, 3H, CH₃CN), 1.84 (s, 3H, CH₃CO), 3.09 (m, 2H, NCH₂), 4.81 (s, 1H, COCHCN), 10.88 (s, 1H, NH). ¹³C NMR (100 MHz, CDCl₃) δ_{C} 13.59 (CH₃CH₂), 18.66 (CH₃CN), 19.87 (CH₃CO), 28.58, 31.98, 42.57 (CH₂CH₂CH₂NH), 94.84 (COCHCN), 163.03 (CH₃CN), 194.42 (CH₃CO). FT-IR: 3284 cm⁻¹ [NH], 1608 cm⁻¹ [CO]. MS (EI, 70 eV) m/z 155 [HL].

[CH₃C(NCH(CH₃)₂)CH₂C(O)OCH₂CH₃] (2). To a three-necked flask was added 30 mL (0.235 mol) of ethylacetoacetate. Next, isopropylamine (20 mL, 0.235 mol) was added *via* a syringe. The mixture was heated to reflux for 1 h. Next, 20 mL of diethyl ether was added and the solution was dried over magnesium sulfate. After filtration, the diethyl ether was evaporated *in vacuo*, affording a viscous, light yellow liquid which was vacuum distilled to give **2** as a colorless liquid (36.2 g, 90.2% yield). bp (78.5 °C, 2.8 mmHg). ¹H NMR (400 MHz, CDCl₃) δ_{H} 1.16 (d, 6H, (CH₃)₂CH), 1.21 (t, 3H, CH₃CH₂), 1.90 (s, 3H, CH₃C), 3.64 (m, 1H, (CH₃)₂CH), 4.04 (q, 2H, CH₃CH₂), 4.35 (s, 1H, CHCO), 8.40 (s, 1H, NH). ¹³C NMR (100 MHz, CDCl₃) δ_{C} 14.57 (CH₃C), 19.01 (CH₃CH₂), 24.01 ((CH₃)₂CH), 44.33 (CH₂CH₃), 58.06 ((CH₃)₂CH), 81.62 (CHCO), 160.73 (CN), 170.50 (CO). FT-IR: 3272 cm⁻¹ [NH], 1651 cm⁻¹ [CO]. MS (EI, 70 eV): m/z 171 [HL].

[Zn(CH₃C(NCH₂CH₂CH₂CH₃)CHCOCH₃)₂] (3). Under an inert atmosphere of nitrogen, 4-*N* (butylamino)-3-penten-2-one (1.36 g, 8.78 mmol) was added to a Schlenk flask containing 50 mL of dried hexanes and a magnetic stir bar. The mixture was cooled to 0 °C and a 1 M solution of diethylzinc in hexane (4.4 mL, 4.4 mmol) was added dropwise *via* a syringe. The mixture was heated to reflux and stirred for 30 min. After cooling, the solvent was removed *in vacuo* and the product was washed three times with cold pentane to yield **3** as a white solid (1.3 g, 71.43% yield).

mp 72 °C. ¹H NMR (400 MHz, CDCl₃) δ_{H} 0.89 (t, 6H, CH₃CH₂), 1.31 (m, 4H, CH₃CH₂CH₂), 1.45 (m, 4H, CH₂CH₂CH₂), 1.92 (s, 6H, CH₃CN), 1.94 (s, 6H, CH₃CO), 3.24 (m, 4H, NHCH₂), 4.78 (s, 2H, COCHCN). ¹³C NMR (100 MHz, CDCl₃) δ_{C} 13.90 (CH₃CH₂), 19.87 (CH₃CN), 21.67 (CH₃CO), 27.37, 33.02, 50.70 (CH₂CH₂CH₂NH), 96.64 (COCHCN), 172.01 (CH₃CN), 181.84 (CH₃CO). MALDI-TOFMS: m/z 373.21 [ML₂]. Anal. Calcd. for C₁₈H₃₂N₂O₂Zn: C, 57.83; H, 8.63; N, 7.49; Found: C, 57.73; H, 8.46; N, 7.62.

[Zn(CH₃C(NCH(CH₃)₂)CHC(O)OCH₂CH₃)₂] (4). Under an inert atmosphere of nitrogen ethyl 3-isopropylamino-2-butenolate (2.0 g, 12 mmol) was added to a 125 mL Schlenk flask containing 35 mL of hexane and a magnetic stir bar. The mixture was cooled to 0 °C and a 1 M solution of diethylzinc in hexane (5.84 mL, 6 mmol) was added dropwise *via* syringe. The mixture was stirred and heated to reflux for 30 min. After cooling, the solvent was removed *in vacuo*. The isolated product was dissolved in 3 mL of pentane and cooled to -5 °C overnight after which the formation of white crystalline material was observed. The solvent was removed *via* cannulation, and the solid was washed three times with 3–5 mL of cold pentane to afford **4** as a crystalline white solid (1.445 g, 61.02% yield). mp 109 °C. ¹H NMR (400 MHz, CDCl₃) δ_{H} 1.07 (d, 6H, (CH₃)₂CH), 1.08 (d, 6H, (CH₃)₂CH), 1.23 (t, 6H, CH₃CH₂), 2.00 (s, 6H, CH₃C), 3.80 (m, 2H, (CH₃)₂CH), 4.10 (q, 4H, CH₃CH₂), 4.30 (s, 2H, CHCO). ¹³C NMR (100 MHz, CDCl₃) δ_{C} 14.89 (CH₃C), 22.32 (CH₃CH₂), 24.68 ((CH₃)₂CH), 49.68 (CH₂CH₃), 59.12 ((CH₃)₂CH), 77.88 (CHCO), 170.37 (CN), 170.95 (CO). MALDI-TOFMS: m/z 404.22 [ML₂]. Anal. Calcd. for C₁₈H₃₂N₂O₄Zn: C, 53.27; H, 7.95; N, 6.90; Found: C, 53.19; H, 7.84; N, 6.82.

MALDI-TOFMS

The MALDI-TOFMS matrix compound used was *meso*-tetrakis (pentafluorophenyl) porphyrin or F20TPP. The matrix (10 mg, 10.3 μ mol) was dissolved in 1 mL of CH₂Cl₂. A few milligrams of the precursor was dissolved in 2 mL CH₂Cl₂. The precursor solution (20 μ L) was then combined with the matrix solution (80 μ L), and vortexed for a few seconds. This resultant solution (1 μ L) was then spotted onto a 100-well stainless steel MALDI sample plate and allowed to dry before the sample plate was loaded into the MALDI ion source.

X-Ray crystallography

The summaries of crystal data, data collection and refinement parameters for **3** and **4** are listed in Table 2. Single crystals of **3** and **4** were mounted on a glass fiber. The crystal measurements were obtained at 103 K on a Bruker SMART CCD diffractometer with graphite-monochromated MoK α radiation ($\lambda = 0.71073$ Å) with absorption corrections performed using the SADABS program.³³ Re-collection and analysis of the initial 50 frames showed that no decay correction was needed. The structures were solved by direct methods³⁴ and refined on F^2 by full-matrix least-squares using the SHELXL97 program package.³⁵

CCDC reference numbers 600122 and 600123.

For crystallographic data in CIF or other electronic format see DOI: 10.1039/b603308c

Table 1 Selected bond distances (Å) and bond angles (°) for **3** and **4**

	3	4
Zn–O(1A)	1.9424(12)	1.9572(11)
Zn–O(1B)	1.9455(11)	1.9454(11)
Zn–N(1A)	1.9893(14)	1.9475(14)
Zn–N(1B)	1.9836(14)	1.9491(13)
O(1A)–Zn–O(1B)	110.08(5)	110.97(5)
O(1A)–Zn–N(1B)	114.78(5)	110.29(5)
O(1A)–Zn–N(1A)	98.37(5)	96.64(5)
O(1B)–Zn–N(1A)	114.25(5)	111.77(5)
O(1B)–Zn–N(1B)	98.11(5)	97.85(5)
N(1B)–Zn–N(1A)	121.68(6)	129.30(6)

Table 2 Crystal data for complexes **3** and **4**

Compound	3	4
Chemical formula	C ₁₈ H ₃₂ N ₂ O ₂ Zn	C ₁₈ H ₃₂ N ₂ O ₄ Zn
Formula weight	373.83	405.83
Crystal System	Triclinic	Monoclinic
Space group	<i>P</i> $\bar{1}$	<i>P</i> 2 ₁ / <i>n</i>
<i>D</i> _c /g cm ⁻³	1.299	1.313
<i>a</i> /Å	8.0085(6)	7.62808(6)
<i>b</i> /Å	11.0745(9)	14.0222(11)
<i>c</i> /Å	12.4796(10)	19.2161(15)
<i>a</i> /°	67.725(1)	90.00
<i>β</i> /°	84.904(1)	91.473(1)
<i>γ</i> /°	69.131(1)	90.00
<i>V</i> /Å ³ , <i>Z</i>	955.66(13), 2	2052.8(3), 4
<i>T</i> /K	103(2)	103(2)
<i>μ</i> /mm ⁻¹	1.296	1.219
Refls. Collected/unique	7216/4499	15417/5066
<i>R</i> _{int}	0.0181	0.0313
<i>R</i> , <i>wR</i> ₂	0.0286, 0.0693	0.0276, 0.0660

AP-MOCVD

Chemical vapor deposition experiments were carried out utilizing a hot-walled reactor comprising a tube furnace and a quartz tube. Approximately 1 g of the precursor was loaded into an open porcelain boat which was placed inside the portion of the quartz tube that extended outside the furnace. Three silicon substrates were placed inside the portion of the quartz tube that resided in the tube furnace. The side of the quartz tube containing the porcelain boat was equipped with a gas adapter and N₂ was made to flow over the precursor and through the reactor at a rate of 15 sccm. The precursor boat was heated to 225 °C (**3**) or 205 °C (**4**) and the substrate was heated to 450 °C. The reaction was carried out for 120 min over which time the formation of a film was observed on the silicon substrate.

X-Ray photoelectron spectroscopy

The X-ray photoelectron spectroscopy measurements were carried out using Kratos Axis 165 spectrometer at a vacuum of 6 × 10⁻¹⁰ Torr with non-monochromatic Mg K α radiation. The X-ray power used for the measurements was 144 W. Individual region scans (Zn 2p, O 1s and C 1s) were performed in hybrid mode using both electrostatic and magnetic lenses, with a step size of 0.2 eV and sweep time of 60 s. All spectra were recorded in the FAT analyzer mode with a pass energy of 40 eV, and an average of 10 scans. Binding energy was calibrated with respect to C1s at 284.6 eV.

Argon ion milling was carried out at a pressure of 3.2 × 10⁻⁷ Torr for 3 min of etch time. The parameters used for etching were 15 mA and 4 kV. The etching as well as the following XPS measurements were performed on the same spots as before.

Data processing was performed using Vision processing software. After subtraction of a linear background, all spectra were fitted using 60% Gaussian/40% Lorentzian peaks, taking the minimum number of peaks consistent with the best fit. The important parameters used for this fitting were peak position, full width at half maximum, intensity and the Gaussian fraction which determine the fraction of the Gaussian component in the fitted peak shape.

Acknowledgements

The authors would like to acknowledge C. Wolf and Y. Badei for assistance in collecting the elemental analysis data and N. Pickett and B. Varughese for XRD and XPS studies. This work was supported by the FACES career initiation award and the Howard University FRSG program.

References

- R. Groenen, J. Loeffler, J. Linden, R. Schropp and M. van de Sanden, *Thin Solid Films*, 2005, **492**, 298.
- Q. Wan, Q. Li, Y. Chen, T. Wang, X. He, J. Li and C. Lin, *Appl. Phys. Lett.*, 2004, **84**, 3654.
- M. Wang, J. Wang, W. Chen and L. Wang, *J. Mater. Sci.*, 2005, **40**, 5281.
- M. Wu, T. Shiosaki and A. Kawabata, *IEEE J. Quantum Electron.*, 1989, **25**, 252.
- T. Gupta, *J. Am. Ceram. Soc.*, 1990, **73**, 1817.
- J. Park, I. Jung, J. Moon, B. Lee and S. Kim, *J. Cryst. Growth*, 2005, **282**, 353.
- R. Ayouchi, D. Leinen, F. Martin, M. Gabas, E. Dalchiele and J. Ramos-Barrado, *Thin Solid Films*, 2003, **426**, 68.
- N. Benramdane, W. Murad, R. Misho, M. Ziane and Z. Kebbab, *Mater. Chem. Phys.*, 1997, **48**, 119.
- M. Tammenmaa, T. Koskinen, L. Hiltunen, L. Niinisto and M. Leskela, *Thin Solid Films*, 1985, **124**, 125.
- V. Lujala, J. Skarp, M. Tammenmaa and T. Suntola, *Appl. Surf. Sci.*, 1994, **82**, 34.
- T. Shiosaki, S. Ohnishi, Y. Murakami and A. Kawabata, *J. Cryst. Growth*, 1978, **45**, 346.
- T. Hur, Y. Hwang, H. Kim and I. Lee, *J. Appl. Phys.*, 2006, **99**, 64308–1.
- T. Yanagitani, T. Nohara, M. Matsukawa, Y. Wantanabe and T. Otani, *IEEE Trans. Ultrason. Ferroelect. Freq. Contr.*, 2005, **52**, 2140.
- B. Cockayne and P. J. Wright, *J. Cryst. Growth*, 1984, **68**, 223.
- F. Smith, *Appl. Phys. Lett.*, 1983, **43**, 1108.
- J. Auld, D. Houlton, A. Jones, S. Rushworth, M. Azad Malik, P. O'Brien and G. Critchlow, *J. Mater. Chem.*, 1994, **4**, 1249.
- D. Neumayer, J. Belot, R. Feezel, C. Reedy, C. Stern, T. Marks, L. Liable-Sands and A. Rheingold, *Inorg. Chem.*, 1998, **37**, 5625.
- D. Studebaker, D. Neumayer, B. Hinds, C. Stern and T. Marks, *Inorg. Chem.*, 2000, **39**, 3148.
- S. Pasko, L. Hubert-Pfalzgraf, P. Richard and A. Abrutis, *Inorg. Chem. Commun.*, 2005, **8**, 483.
- N. Edleman, A. Wang, J. Belot, A. Metz, J. Babcock, A. Kawaoka, J. Ni, M. Metz, C. Flaschenriem, C. Stern, L. Liable-Sands, A. Rheingold, P. Mackworth, R. Chang, M. Chudzik, C. Kannewurf and T. Marks, *Inorg. Chem.*, 2002, **41**, 5005.
- Y. Liu, Y. Cheng, T. Tung, Y. Chi, Y. Chen, C. Liu, S. Peng and G. Lee, *J. Mater. Chem.*, 2002, **13**, 135.
- S. Lim, B. Choi, Y. Min, D. Kim, I. Yoon, S. Lee and I. Lee, *J. Organomet. Chem.*, 2004, **689**, 224.
- J. Matthews, O. Just, B. Obi-Johnson and W. Rees, Jr., *Chem. Vap. Deposition*, 2000, **6**, 129.

-
- 24 L. Wang, Y. Yang, N. Yu, J. Ni, C. Stern and T. Marks, *Chem. Mater.*, 2005, **17**, 5697.
- 25 J. Matthews, T. Ouattara and R. Butcher, *Acta Crystallogr., Sect. E*, 2005, **61**, m2598.
- 26 T. Ouattara, R. Butcher and J. Matthews, *J. Coord. Chem.*, 2005, **58**, 461.
- 27 W. Rees, Jr., O. Just, S. Castro and J. Matthews, *Inorg. Chem.*, 2000, **39**, 3736.
- 28 U. Patil, M. Winter, H. Becker and A. Devi, *J. Mater. Chem.*, 2003, **13**, 2177.
- 29 R. Bhakta, F. Hipler, A. Devi, S. Regnery, P. Ehrhart and R. Waser, *Chem. Vap. Deposition*, 2003, **9**, 295.
- 30 D. Schulz, B. Hinds, D. Neumayer, C. Stern and T. Marks, *Chem. Mater.*, 1993, **5**, 1605.
- 31 L. Wang, Y. Yang, J. Ni, C. Stern and T. Marks, *Chem. Mater.*, 2005, **17**, 5697.
- 32 J. Ni, H. Yan, A. Wang, Y. Yang, C. Stern, A. Metz, S. Jin, L. Wang, T. Marks, J. Ireland and C. Kannewurf, *J. Am. Chem. Soc.*, **127**, 5613.
- 33 G. Sheldrick, *SADABS, Program for Empirical Absorption Correction of Area Detector Data*, University of Göttingen, Germany, 1996.
- 34 G. Sheldrick, *SHELXS-97, Program for Crystal Structure Solution*, University of Göttingen, Germany, 1997.
- 35 G. Sheldrick, *SHELXL-97, Program for Crystal Structure Refinement*, University of Göttingen, Germany, 1997.